COMPDYN 2011
III ECCOMAS Thematic Conference on
Computational Methods in Structural Dynamics and Earthquake Engineering
M. Papadrakakis, M. Fragiadakis, V. Plevris (eds.)
Corfu, Greece, 25–28 May 2011

DISTURBANCE SOURCES MODELING FOR ANALYSIS OF STRUCTURE-BORNE MICRO-VIBRATION

G.S Aglietti[1], Z. Zhang[1], G Richardson[2], B. Le Page[2], A Haslehurstl[2]

[1]School of Engineering Science, University of Southampton,
Highfield, Southampton, SO17 1BJ, UK
gsa@soton.ac.uk

[2] Surrey Satellite Technology Limited,
Guildford, Surrey, UK

Keywords:.

Abstract. *Micro-vibration is a low level disturbance, which cannot be controlled or reduced by the Attitude and Orbit Control System of a spacecraft. It can emanate from various sources on a typical spacecraft, notably subsystems with moving parts such as reaction wheels or cooler mechanisms. Micro-vibration can also result from thermo-elastic effects due to stick-slip from differential expansion of parts. It causes problems for sensitive payloads especially high resolution cameras where the demand for higher resolution (which drives stability requirements), has made analysis and control of microvibrations relevant for a larger number of satellites. The availability of mathematical models to represent the disturbance sources in a format that can themselves be coupled to the mathematical model of the structure to perform end-to-end analysis to obtain predictions of the stability level at the receiver is crucial.*

In the simplest form the sources can be represented with forces and moments of appropriate characteristics, adding also some inertia at the source location. But even for this simplistic implementation it is necessary to have available the details of the forces and moment produced by a source, and these can be either calculated from schematic models of the functioning of the device, or experimentally determined, or a mixture of the two. Typical test techniques applied to micro-vibration measurement /characterization will be described, highlighting advantages and drawbacks of the various methods. A simple experimental apparatus for the measurement of the micro-vibrations emitted by a reaction wheel is presented. A mathematical model of the reaction wheel disturbances is also presented together with its coupling to a typical spacecraft structural model.

1 INTRODUCTION

Since the early 1990's, the resolution and pointing stability required for Earth and deep space astronomical observation spacecraft instruments have continuously increased. Current high resolution military reconnaissance satellites have achieved centimeter-level ground resolution. For example, the KH-13 surveillance satellite recently launched has reached a ground resolution of 0.05 m. Space telescopes for astronomical observations usually have a resolution one to two orders of magnitude higher than Earth observation satellites [1], and looking at the future, the James Webb Space Telescope (JWST) planned to launch in 2014 or 2015 should reach a pointing stability 0.004 arcsec [2].

On board satellites there is often equipment (e.g. Reaction & Momentum Wheel Assemblies, Cryocoolers, pointing mechanisms, switches etc) in this context called sources, which during their functioning produce dynamic disturbances, micro-vibrations that are transmitted through the platform affecting the performance of sensitive payloads receivers also mounted on the platform. The micro-vibration produced by the sources can also be amplified by structural resonances thus making micro-vibration prediction complicated.

In this context, the term micro-vibration refers to low-level mechanical disturbances in the range of micro-g's (μg), typically occurring at frequencies from a few Hz up to 1000 Hz [3]. In some extreme cases of high precision spacecraft [4-6] even disturbances at frequencies down to 10-2 Hz are relevant. Micro-vibration can be considered as excitations resulting from impulsive phenomena (device release); translating parts (cryocoolers); or rotating parts (RWAs/MWAs), for example, which are sinusoidal (or multi-tone) or broad band frequency in nature.

Generally speaking, micro-vibration sources exist on most spacecraft; however, due to their small amplitudes and often high frequencies they do not have serious impacts (e.g. typical satellites for telecommunication) and thus are ignored. Spacecraft with optical instruments and cameras are generally those most affected by micro-vibration issues. Micro-vibration generally cannot be controlled or reduced by the Attitude and Orbit Control System (AOCS) because they usually involve the flexible modes of the spacecraft structure (rather than its rigid body motion, which is controlled by the AOCS) and because the frequency range of the spacecraft AOCS usually has an upper limit of controllable frequency of a few Hz, whereas micro-vibration generally occurs at higher frequencies.

Micro-vibration can be managed passively and/or actively at the source, along the transmission path and at the receiver location. For example, in order to reduce disturbances, RWAs can be placed on a vibration isolation mount [7] or bracket [8] which is connected to the primary structure, micro-vibration isolators can be incorporated in to primary structure components [9], and/or active optics such as an image stabilization system used within optical payloads [10]. Passive or active isolation may also be used between the receiver and the spacecraft structure.

2 MICRO-VIBRATION NOISE SOURCES

Micro-vibration disturbances mainly arise from fast moving (rotating and translating) mechanisms installed onboard such as RWAs, cryocoolers and pointing systems, etc. [11]. They may also arise from non-moving systems such as electronics and sensors [12], the release of strain energy at structural interfaces (joints, latches, hinges) during "thermal snap" events [13, 14] and the bending of solar arrays, antennas, etc. due to sudden temperature change [15].

The mechanical disturbances produce by the noise sources are usually characterized by forces and torques that appear at the interface between the equipment and spacecraft. These forces/torques propagate through the primary structure to the sensitive instruments. Since the spacecraft is an isolated system, the mechanical energy produced by these excitations must be dissipated into this system.

Generally micro-vibration sources can be divided into two broad groups:

- Single disturbance event
- Continuous disturbances.

The single disturbance event, also known as transient loads, are clanks and intermittent disturbances, which may occur randomly (sudden stress release due to slippage between parts with differential temperatures and/or thermal expansion of their materials; micro-cracking in laminates and sandwiches; and buckling of foils due to thermal expansion/contraction) or at specified commands (for example firing a thruster). These disturbances are low level shock type forces with small dynamic amplitudes.

The continuous disturbances, also known as vibratory loads, are accelerations which are sinusoidal (or multi-tone) or broad band frequency in nature. The continuous disturbance can be further broken down based on the speed, magnitude and noise source type. For example, based on the first criteria high speed moving mechanisms include RWAs/MWAs, gyros, etc.; medium ones include liquid flowing and sloshing, cryocoolers, etc and low speed ones include antennas, solar arrays, etc. Based on the second criteria, mechanical mechanism induced disturbances include those mentioned above except those induced from liquid flowing and sloshing, which are regarded as non-mechanical mechanisms. Either way, these sources produce permanent disturbances in spacecraft, and are usually considered as “internal noise” [1, 12]. Other possible disturbances include inductive electromagnetic forces between wires and heaters; electrical noise, etc.

2.1 Physical causes of micro-vibrations

Within the noise sources micro-vibration arises from common mechanical components or phenomenon. These are summarized below

- Rotor imbalance: Rotating devices such as RWA, MWA, gyroscope, etc. can pro-duce large disturbances in spacecraft, especially when spin speed is very high. At nominal high speed, rotor imbalance is considered as the major disturbance source in these devices. It cannot be totally avoided because of manufacturing tolerances. Usually rotor imbalance is con-

sidered as the sum of static and dynamic imbalance, both of which produce disturbance forces and torques. These forces and torques are proportional to spin speed squared with a fundamental frequency equal to spin speed.

- Mechanical bearing irregularity: Disturbances caused by mechanical bearing irregularity are mainly due to ball irregularities; internal race irregularities; external race irregularities and cage disturbances. These are also due to manufacturing tolerances. For high speed continuous rotation devices such as brushless DC motor and stepper motor, interactions between them, e.g. abnormal contacts between balls and raceway, balls and cage, cage and raceways, create non-linear disturbance force and torque, they appear as sub- and super-harmonics in the device disturbance signature.

- Bearing friction: Bearing friction occurs in all rotating devices through their entire operational range, but it is particularly important at low speed. If a device needs to reverse directions (crossing zero speed), e.g. an RWA, there are two disturbance possibilities either the device will stop rotating briefly (there will be a dead band) or there will be a discontinuity in acceleration (due to the change in the relative signs of the friction and motor torque).

- lubrication degradation: In rotating devices, such as RWA and SADM, lubrication degradation over life can lead to increased noise or as is with some systems using a sacrificial liberation system can change the noise performance during life as the cages wears or can lead to periodic high torque (noise).

- Motor cogging, Motor ripple: For a permanent magnet brushless DC motor, motor disturbances include cogging and torque ripple. These disturbances generally only be-come significant when wheel speed is low or the motor reverses spin direction. Motor cogging torque originates from the magnetic interaction between stator slots and rotor permanent magnets, and it is an undesirable effect that prevents the smooth rotation of the flywheel and results in noise. Motor ripple torque is defined as the change in mo-tor torque with respect to the angular position, or simply by the profile of the Back-Electro Motive Force (B-EMF) and current waveform, which is not exactly sinusoidal.

- Stepper motors, gear meshing and contact: For APMs, usually two or three phase stepper motor actuators are used to drive antenna in two axes (azimuth and elevation), respectively. Each actuator step imparts a small disturbance torque into the spacecraft. Also gear meshing and contacts are also sources of vibration.

- Axial motion of inertias, such as the compressor and other moving parts in a cryocooler can become sources of vibration [16]. The linearly reciprocating motion of the elements gives rise to a momentum imbalance. Particularly for cryocoolers the piston is typically driven with a sinusoidal signal, it oscillates against a non-linear gas spring formed by the compression space, resulting in a non-sinusoidal piston motion. A disturbance of this type manifests itself in the vibration signature as the presence of harmonics of the moving inertia's drive frequency [17].

As rotor imbalance is one of the main causes of microvibrations this article focuses on the modeling of this phenomena and its integration with a structural model of the satellite.

3 MATHEMATICAL MODEL

The wheel imbalance typically consists of the flywheel static imbalance (offset of the center of mass (CoM) of the flywheel with respect to its spin axis) and dynamic imbalance (misalignment of the flywheel's principal axis and the rotation axis). The wheel-induced vibrations are mostly sinusoidal (often multi-tone) in nature, and below the first resonant frequency, the imbalance causes a disturbance force and moment respectively at the flywheel's spin rate (the fundamental harmonic) with amplitude proportional to the rotational speed squared.

Common flywheel configurations of a WA are either symmetrical (flywheel at mid-span of the shaft) or cantilevered (flywheel at one end of the shaft), see Fig. 1. Flywheel imbalance analytical models of such configurations have been studied in the literature.

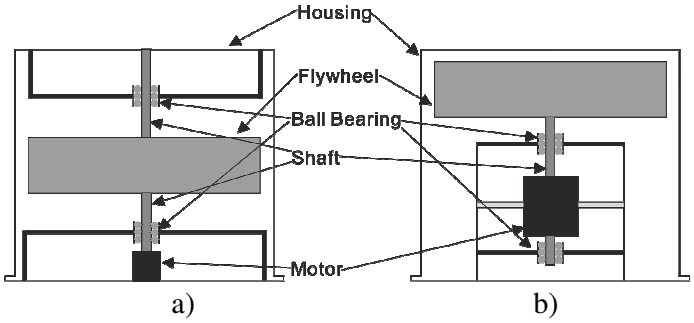

Fig. 1 Two typical RWA configurations a) symmetrical b) cantilever

In this article, the WA studied has a cantilevered flywheel supported by a soft suspension system, which provides both rotational and translational support (see Fig. 2). The soft suspension system is designed as a passive system that filters the vibrations produced by the motor (e.g. its bearings), thus minimizing the mechanical disturbances emitted by the WA when spinning. Also the WA is designed to have a speed range beyond 10000 rpm, making it suitable for use as either a RWA or MWA.

Based on the energy method (i.e. the Lagrange's approach), the flywheel imbalance analytical model of the wheel is coupled with an arbitrary supporting structure (in this case, an aluminum ”cube” acting as a seismic mass), see Fig. 2. The analytical model representing the flywheel imbalance can then be integrated with disturbance empirical models (i.e. the semi-empirical models) and linked to a complete satellite numerical model to predict its performance at the receivers’ location (e.g. the effect on the line of sight of an optical instrument).

The whole system (WA and seismic mass, which also includes the wheel base) is suspended using elastic cords on each side of the seismic mass, thus simulating a “free-free” condition. The elastic cords were chosen such that the system resonant frequency is less than 1 Hz (verified with a “tap” test), and not in the frequency range interested in this article.

The seismic mass has coordinate $x_c y_c z_c$ with origin C at its CoM; θ_c, φ_c and ψ_c are the corresponding rotations around each axis. Note that, in the shaft pointing direction, the kinetic energy of the wheel is much larger than that of the seismic mass, thus the perturbation of the seismic mass about this axis, ψ_c is ignored. M_c is the mass of the seismic mass; I_{c_xx} and I_{c_yy} are moment of inertias of the seismic mass about x_c and y_c axis respectively. The vertical distance from the soft suspension system-wheel base interface to the CoM of the seismic mass is l.

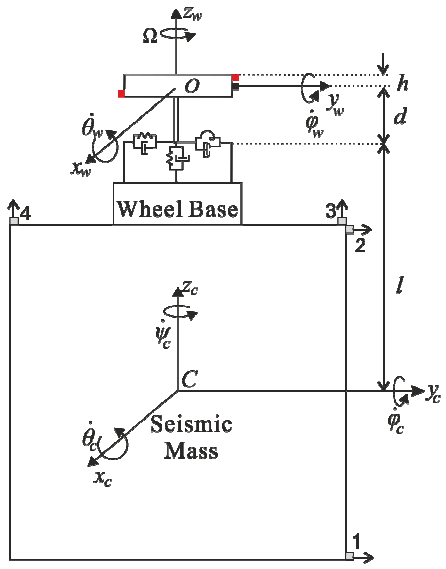

Fig. 2 Simplified model of reaction Wheel coupled with seismic mass

The seismic mass can be considered as a rigid body connected with a flywheel (another rigid body) by the soft suspension system. With small displacement assumption, the kinetic energy of the seismic mass T_c is obtained as:

$$T_c \approx \frac{1}{2}\left[M_c\left(\dot{x}_c^2+\dot{y}_c^2+\dot{z}_c^2\right)+I_{c\_xx}\dot{\theta}_c^2+I_{c\_yy}\dot{\varphi}_c^2\right] \tag{1}$$

The potential energy U_s of the system can be obtained (using the small displacement assumption) through the relative motion at the soft suspension system/flywheel base interface:

$$U_s=\frac{1}{2}\left[k_z\left(z_w-z_c\right)^2+k_r\left(\theta_w-\theta_c\right)^2+k_t\left[\left(y_w-y_c\right)+\left(d\theta_w+l\theta_c\right)\right]^2+k_r\left(\varphi_w-\varphi_c\right)^2+k_t\left[\left(x_w-x_c\right)-\left(d\varphi_w+l\varphi_c\right)\right]^2\right] \tag{2}$$

The fully linearized EoMs of the system with respect to each of the ten DoFs (the axial rotation of flywheel and seismic mass are not included) are obtained. They are written in matrix form as:

$$\boldsymbol{M}_s\ddot{\boldsymbol{q}}_s+\boldsymbol{G}_s\dot{\boldsymbol{q}}_s+\boldsymbol{K}_s\boldsymbol{q}_s=\boldsymbol{F}_s \tag{3}$$

The mathematical model was validated against test results, and various tests were carried out to validate the effect of the stiffness of the mechanism supporting the rotor.

In particular Figure 3 shows a comparison of waterfall plot for the in-plane force emitted by the wheel for tow cases a soft suspension system, and a rigid one. It is possible to notice that the rigid assembly emits considerable more vibration in the frequency range between 200Hz and 400Hz.

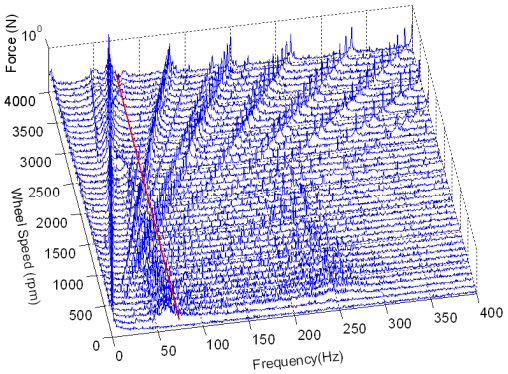

a) Disturbance force in *y* direction of flexible WA

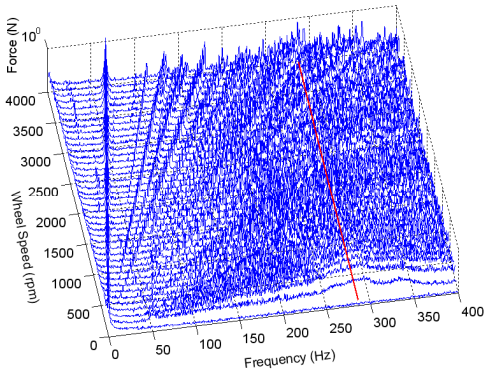

b) Disturbance force in *y* direction of rigid WA

Fig.3 Waterfall plots for flexible and rigid WA

4 SOURCE-STRCUTRE INTEGRATION

Measured interface disturbance force and torque generated by mechanisms need to be integrated with the spacecraft model in order to assess performance at receivers. Methods of disturbance source implementation vary depending on the source and spacecraft model type, i.e. sources could be analytical, empirical or semi-analytical, the spacecraft model could be FE model or Matlab/Simulink model. The most common method is to implement semi-analytical source models and integrate them in typical spacecraft FE model (whose behavior is described using its transfer functions). Typically, this can be described mathematically as:

$$\boldsymbol{Z} = \boldsymbol{G}\boldsymbol{W} \tag{4}$$

where $\boldsymbol{Z}$ is the performance metrics at some point, such as displacement or acceleration at the receivers. $\boldsymbol{G}$ is the transfer function matrix between the receivers and sources, usually obtained from the spacecraft FE model. W is the disturbance sources. Eq. (4) is most often written into spectral density form:

$$\boldsymbol{\Phi}_{ZZ} = \boldsymbol{G}\boldsymbol{\Phi}_{FF}\boldsymbol{G}^{H} \tag{5}$$

where $\boldsymbol{\Phi}_{FF}$ is the measured disturbance in spectral density matrix form - usually a 6×6 matrix in the form:

$$\boldsymbol{\Phi}_{FF} = \begin{bmatrix} \Phi_{F_x} & \Phi_{F_xF_y} & \Phi_{F_xF_z} & \Phi_{F_xM_x} & \Phi_{F_xM_y} & \Phi_{F_xM_z} \\ \Phi_{F_yF_x} & \Phi_{F_y} & \Phi_{F_yF_z} & \Phi_{F_yM_x} & \Phi_{F_yM_y} & \Phi_{F_yM_z} \\ \Phi_{F_zF_x} & \Phi_{F_zF_y} & \Phi_{F_z} & \Phi_{F_zM_x} & \Phi_{F_zM_y} & \Phi_{F_zM_z} \\ \Phi_{M_xF_x} & \Phi_{M_xF_y} & \Phi_{M_xF_z} & \Phi_{M_x} & \Phi_{M_xM_y} & \Phi_{M_xM_z} \\ \Phi_{M_yF_x} & \Phi_{M_yF_y} & \Phi_{M_yF_z} & \Phi_{M_yM_x} & \Phi_{M_y} & \Phi_{M_yM_z} \\ \Phi_{M_zF_x} & \Phi_{M_zF_y} & \Phi_{M_zF_z} & \Phi_{M_zM_x} & \Phi_{M_zM_y} & \Phi_{M_z} \end{bmatrix} \tag{6}$$

where diagonal Φ_{ii} are the PSD, Φ_{ij} are the CSD. The spectral matrix $\mathbf{\Phi}_{FF}$ is the input in the spacecraft FE model.

Methods to obtain the $\mathbf{\Phi}_{FF}$ are usually empirical test results or a semi-analytical model.

For the first method, for every speed, disturbance force and moment $\mathbf{F}(\omega)$ in frequency domain at the mechanism interface is obtained through load cell or Kistler table, i.e. a 6×1 vector.

$$\boldsymbol{F}(\omega) = \begin{Bmatrix} F_x \\ F_y \\ F_z \\ M_x \\ M_y \\ M_z \end{Bmatrix} \tag{7}$$

This vector is then converted into spectral density matrix (Eq. (6)) utilizing signal processing technique, which can then be used in Eq. (5).

The second methods involves semi-analytical model of disturbance. In general, wheel imbalance induced disturbance has the analytical form of:

$$F(t) = \sum_{i=1}^{n} C_i f_{rwa}^2 \sin\left(2\pi h_i f_{rwa} t + \phi_i\right) + W(t) \tag{8}$$

where $F(t)$ is the disturbance force or torque in time domain; n is the number of harmonics; C_i is the amplitude of the i_{th} harmonic; f_{rwa} is the flywheel speed rate in Hz; h_i is the i^{th} harmonic number and ϕ_i is a random phase; $W(t)$ is the random noise disturbance.

Note Eq. (8) is an alternative form of the excitation, i.e. right hand side, of the Eq. (3). From Eq. (8), parameters for each harmonic and the number of harmonics need to be mapped from experimental data (i.e. empirical results) for each speed (the choice of these values depends on the accuracy of the model want to obtained). And high frequency random (white) noise has to be generated and incorporated with the model. Once the disturbance force and moment in time domain obtained, they can processed into frequency domain to obtain $\mathbf{F}(\omega)$, the following analysis becomes the same as the first method.

5 CONCLUSIONS

In this article, the importance of microvibrations modeling has been briefly discussed to highlight its importance in the design of high stability satellite platforms. The various physical mechanisms that produce microvibrations on board a typical satellite have been reviewed and

a mathematical model of a typical source, i.e. a reaction wheel, has been described. Finally the article describes a possible method to introduce the loads produced by the source(s) in a model describing the structure transfer functions, which could be obtained using any modeling technique such as the Finite Element Method.

REFERENCES

[1]. Zhang, Z., Yang, L., and Pang, S. "Jitter Environment Analysis for Micro-precision Spacecraft," *Spacecraft Enviroment Engineering* Vol. 26, No. 6, 2009, pp. 528-534.

[2]. Meza, L., Tung, F., Anandakrishnan, S., Spector, V., and Hyde, T. "Line of Sight Stabilization of James Webb Space Telescope," *27th Annual AAS Guidance and Control Conference*. AAS 05-002, Breckenridge, CO, 2005.

[3]. Bely, P. Y., Lupie, O. L., and Hershey, J. L. "The Line-of-sight Jitter of the Hubble Space Telescope," *Space Astronomical Telescopes and Instruments II*. 1 ed. Vol. 1945, SPIE, Orlando, FL, USA, 1993, pp. 55-61.

[4]. Aglietti, G., Langley, R., Rogers, E., and Gabriel, S. "Model Building and Verification for Active Control of Microvibrations with Probabilistic Assessment of the Effects of Uncertainties," *Proceedings of the Institution of Mechanical Engineers, Part C: Journal of Mechanical Engineering Science* Vol. 218, No. 4, 2004, pp. 389-399.

[5]. Katsukawa, Y., Masada, Y., Shimizu, T., Sakai, S., and Ichimoto, K. "Pointing Stability of Hinode and Requirements for the Next Solar Mission Solar-C," *International Conference on Space Optics*. Rhodes, Greece, 2010.

[6]. Pierrart, C., Clerc, C., Eaton, D. G., and Lefevre, Y. M. "Microvibration Transmission in Space Structures at Medium High Frequencies," *Spacecraft Structures and Mechanical Testing Conference*. Paris, France, 1994.

[7]. Kamesh, D., Pandiyan, R., and Ghosal, A. "Modeling, Design and Analysis of Low Frequency Platform for Attenuating Micro-vibration in Spacecraft," *Journal of Sound and Vibration* Vol. 329, No. 17, 2010, pp. 3431-3450.

[8]. Shankar Narayan, S., Nair, P. S., and Ghosal, A. "Dynamic Interaction of Rotating Momentum Wheels with Spacecraft Elements," *Journal of Sound and Vibration* Vol. 315, No. 4-5, 2008, pp. 970-984.

[9]. Vaillon, L., and Philippe, C. "Passive and Active Microvibration Control for Very High Pointing Accuracy Space systems," *Smart Materials and Structures* Vol. 8, No. 6, 1999, p. 719.

[10]. Sakurai, T. *The Hinode Mission*: Springer, 2008.

[11]. Laskin, R. A., and Martin, M. S. "Control/Structure System Design of a Spaceborne Optical Interferometer," *Proceedings of AAS/AIAA Astrodynamics Specialist Conference*. AAS 89-424, 1989, pp. 369-395.

[12]. Wacker, T., Weimer, L., and Eckert, K. "GOCE Platform Micro-vibration Verification by Test and Analysis," *Proceedings of the European Conference on Spacecraft Structures, Materials and Mechanical Testing*. Noordwijk, The Netherlands, 2005.

[13]. Ingham, M. D. "Microdynamics and Thermal Snap Response of Deployable Space Structures," *Department of Aeronautics and Astronautics*. Vol. M.Sc., Massachusetts Institute of Technology Cambridge, MA, 1995, p. 187.

[14]. Ingham, M., Kim, Y., Crawley, E., McManus, H., and Miller, D. "Experimental Characterization of Thermal Creak Response of Deployable Structures," *Journal of Spacecraft and Rockets* Vol. 37, No. 3, 2000.

[15]. Foster, C. L., Tinker, M. L., Nurre, G. S., and Till, W. A. "The Solar-array-induced Disturbance of the Hubble Space Telescope Pointing System," *Journal of Spacecraft and Rockets* Vol. 32, No. 4, 1995, pp. 634-644.

[16]. Jedrich, N., Zimbelman, D., Turczyn, M., Sills, J., Voorhees, C., and Clapp, B. "Cryo Cooler Induced Micro-Vibration Disturbances to the Hubble Space Telescope," *The 5th Cranfield Dynamics and Control of Systems and Structures in Space Conference*. Cambridge, UK, 2002.

[17]. Collins, S. A. "Multi-axis Analog Adaptive Feedforward Cancellation of Cryocooler Vibration," *Department of Aeronautics and Astronautics*. Vol. Ph.D, Massachusetts Institute of Technology, Cambridge, MA, 1994, p. 222.